STEADY AND DYNAMIC CHARACTERISTICS OF WIDE SLIDER BEARINGS:OPTIMAL-LOAD CONSIDERATION

Jaw-Ren Lin*, Ming-Hsiung Ho, Chi-Yi Chang, Chi-Ren Hung

Department of Mechanical Engineering
Nanya Institute of Technology
Jhongli, Taiwan

Abstract

Finding the optimal load-carrying capacity and understanding the resulting dynamic behavior play important roles in slider-bearing designing. Considering the film-gap height varying slowly with the sliding direction, the optimal-load designing together with the corresponding dynamic characteristics of wide slider bearings is theoretically analyzed in the present study. By applying the technique of calculus of variation, the optimization is performed over a class of stepped bearings with certain shoulder height parameter and riser location parameter. Comparing with the three cases of the plane bearing, the parabolic bearing and the composite bearing, the stepped-profile bearing designed at the optimal shoulder height parameter and riser location parameter provides an enhancement in the load-carrying capacity, a reduction in the friction parameter as well as an improvement in the stiffness characteristics. This optimal-load condition and the corresponding dynamics provide useful information for engineers in bearing selection and reducing power loss.

Key Words: optimal-load designing, calculus of variation, dynamic characteristics, slider bearing, stepped bearing

*E-mail: jrlin@nanya.edu.tw Fax: 03-4384670 Tel: 03-4361070 ext. 6302

寬滑塊軸承軸承之定常態與動態性能：最佳負荷能力考慮

林昭仁　何明雄　張志毅　洪啟仁

南亞技術學院　機械工程系

摘要

找出最佳負荷能力與了解相對應之動態特性，於滑塊推力軸承設計與節省能源要求上扮演很重要之地位。在考慮油膜間隙隨滑動方向變化之情況下，本文主要探討寬滑塊軸承之最佳負荷能力設計並且分析相對應之動態性能。藉由變分學原理之技巧，可分析得到最佳化條件發生在步階軸承之某個肩部高度與步階位置處。若與傾斜平面軸承、拋物線軸承及複合軸承等三種型態做比較，步階軸承在最佳化肩高參數與步階參數之設計下可以得到最佳之負荷能力與最低之摩擦參數，同時亦可提高動相對應之動態剛度性能。整體而言，本文分析所得最佳化條件之參數對於工程師在軸承組件選擇與節省動力能源之考慮上，提供了一個非常有用之參考依據。

關鍵詞: 最佳負荷設計，變分學，動態特性，滑塊軸承，步階軸承

1. Introduction

Load capacities carried by the journal-bearing system possess components acting in the direction of the journal's axis of rotation. Slider bearings are designed therefore to support these thrust loads. Since the geometrical forms of the thrust pad may affect the load of slider bearings, many researches concerning with different film shapes have been made by Pinkus and Sternlicht [11], Cameron [1] and Hamrock [3]. Taking into account various operating conditions further studies are presented, such as the effects of convective inertia forces by Launder and Leschziner [5] and Synder [16], the effects of viscosity-film dependence by Qvale and Wiltshire [12], the effects of turbulent flows by King and Taylor [4] and Taylor and Dowson [17], the effects of thermal and inertia effects by Chowdhury and Ahmadi [2], Rodkiewicz and Anwar [13], Rodkiewicz et al. [14], Safar [15] and Talmage and Carpino [18]. These contributions concentrate upon slider bearings operating at the steady-state condition. To prevent bearing-pad contact, understanding dynamic characteristics of slider bearings receives great important. Recently, studies of dynamic stiffness and damping characteristics of wide slider bearings are made respectively for the plane bearings by Lin et al. [7], the parabolic bearings by Lin et al. [8], the Rayleigh step bearings by Lu et al. [9] and the composite bearings by Lin et al. [10]. According to the results obtained, the steady-state performance and the dynamic characteristics are significantly affected by the inlet-outlet film ratio and the geometric parameter of film shapes. However, in engineering application the optimum wide slider bearing that producing the largest steady-state load-carrying capacity should be specified. Therefore, a further insight into the optimal design for the bearings is of interest.

In the present study, we are mainly concerned with both of the steady and dynamic characteristics of wide slider bearings under the optimal-load designing. By applying the technique of calculus of variation, the optimal film profile of curved sliders is determined. Comparing with the cases of the plane profile, the parabolic profile, the composite profile and the stepped profile, the steady-state performance and the dynamic characteristics of the bearing under the optimal condition are presented in terms of the load-carrying capacity, the friction parameter, the dynamic stiffness coefficient and the damping coefficient.

2. Formulation

The geometrical configuration of a wide slider bearing with a curved profile is described in Figure 1, in which the film thickness varies slowly. The sliding velocity of the lower surface is U, the squeezing velocity of the upper surface is $\partial h / \partial t$, and the film thickness is described by:

$$h(x,t) = h_s(x) + h_m(t) \tag{1}$$

where $h_s(x)$ is the shape function of the film depending the coordinate x, and $h_m(t)$ is the minimum film thickness depending upon the time t. According to the thin-film theory of hydrodynamic lubrication, the dynamic Reynolds-type equation taking into account the squeezing effects is expressed by Lin et al. [7] as:

$$\frac{\partial}{\partial x}(h^3\frac{\partial p}{\partial x}) = 6\mu U\frac{\partial h}{\partial x} + 12\mu\frac{\partial h}{\partial t} \tag{2}$$

where p is the film pressure , and μ is the lubricant viscosity. Expressed in a non-dimensional form one has the dimensionless dynamic Reynolds-type equation.

$$\frac{\partial}{\partial x^*}\left[h^*(x^*,t^*)^3\frac{\partial p^*}{\partial x^*}\right] = 6\frac{\partial h^*}{\partial x^*} + 12\frac{\partial h^*}{\partial t^*} \tag{3}$$

$$h^*(x^*,t^*) = h_s^*(x^*) + h_m^*(t^*) \tag{4}$$

The non-dimensional variables are defined by

$$x^* = \frac{x}{L},\ t^* = \frac{Ut}{L},\ h_s^* = \frac{h_s}{h_{m0}},\ h_m^* = \frac{h_m}{h_{m0}},\ h^* = \frac{h}{h_{m0}},\ p^* = \frac{ph_{m0}^{*\ 2}}{\mu UL} \tag{5}$$

where h_{m0} is the steady minimum film height. To obtain the steady performance and the dynamic characteristics, the upper surface is assumed to undergo a small-amplitude oscillation about its equilibrium position. The minimum film thickness and the film pressure are then perturbed as:

$$h_m^* = 1 + \varepsilon e^{it*},\qquad p^* = p_0^* + p_1^*\varepsilon e^{it*} \tag{6}$$

Substituting into the dimensionless dynamic Reynolds-type equation and neglecting higher-order terms of ε, one obtains the steady Reynolds-type equation and the perturbed Reynolds-type equation, respectively.

$$\frac{\partial}{\partial x^*}\left[(h_s^*+1)^3\frac{\partial p_0^*}{\partial x^*}\right] = 6\frac{dh_s^*}{dx^*}\qquad \text{(steady)} \tag{7}$$

$$\frac{\partial}{\partial x^*}\left[(h_s^*+1)^3\frac{\partial p_1^*}{\partial x^*} + 3(h_s^*+1)^2\frac{\partial p_0^*}{\partial x^*}\right] = 12i\qquad \text{(perturbed)} \tag{8}$$

3. Optimal Analysis and Bearing Characteristics

Integrating the steady Reynolds-type equation (7) once yields

$$\frac{dp_0^*}{dx^*} = F_1(h_s^*) - A_1F_2(h_s^*) \tag{9}$$

where A_1 is the integration constant and

$$F_1(h_s^*) = \frac{6h_s^*}{(h_s^*+1)^3},\ F_2(h_s^*) = \frac{1}{(h_s^*+1)^3} \tag{10}$$

Integrating again with the boundary condition $p_0^*(x^*=0)=0$ leads to

$$p_0^* = \int_0^{x*} F_1(h_s^*)dx^* - A_1\int_0^{x*} F_2(h_s^*)dx^* \tag{11}$$

Using the other boundary condition $p_0^*(x^*=1)=0$, the integration constant A_1 is obtained.

$$A_1 = \int_0^1 F_1(h_s^*)dx^* / \int_0^1 F_2(h_s^*)dx^* \tag{12}$$

Integrating the steady pressure over the film region of length L and width B results in the load-carrying capacity.

$$W_0^* = \frac{W_0 h_{m0}^2}{\mu U L^2 B} = -\int_0^1 F_1(h_s^*)dx^* + A_1\int_0^1 F_2(h_s^*)dx^* \tag{13}$$

By applying the technique of calculus of variation as Lin [6] and Verma et al. [19] and, the optimal design of the wide porous slider bearing can be determined. Let h_s^*, A_1 and W_0^* be changed respectively to $h_s^* + \delta h_s^*$, $A_1 + \delta A_1$ and $W_0^* + \delta W_0^*$, in which δh_s^*, δA_1 and δW_0^* are small quantities of first order. Then equations (12) and (13) change to

$$(A_1 + \delta A_1)\int_0^1 [F_2 + (dF_2 / dh_s^*)\delta h_s^*]dx^* = \int_0^1 [F_1 + (dF_1 / dh_s^*)\delta h_s^*]dx^* \tag{14}$$

$$W_0^* + \delta W_0^* = (A_1 + \delta A_1)\int_0^1 [F_2 + (dF_2 / dh_s^*)\delta h_s^*]x^* dx^* - \int_0^1 [F_1 + (dF_1 / dh_s^*)\delta h_s^*]x^* dx^* \tag{15}$$

Solving equations (12), (13), (14) and (15) and neglecting high-order quantities, one can obtain

$$\delta W_0^* = \int_0^1 \left[\frac{dF_2}{dh_s^*} - A_1\frac{dF_2}{dh_s^*}\right]\left[\int_0^1 F_2 x^* dx^* / \int_0^1 F_2 dx^* - x^*\right]\delta h_s^* dx^* \tag{16}$$

Inspecting the above equation it is found that a stepped film profile could meet the requirement of optimal load-carrying capacity. Recently, both the steady performance and the dynamic characteristics of stepped bearings have been analyzed by Lu et al. [9]. However, the optimal design is not shown. To obtain the optimal load-carrying capacity and the corresponding dynamics, the stepped slider bearing is reconsidered in Figure 2.

Since the film shape on the upper stepped surface is $h_s^*(x^*) = d / h_{m0} = \beta$ for $0 \le x^* \le \alpha$, equations to find the critical riser location parameter α_{cr} and the critical shoulder height parameter β_{cr} are

$$\alpha_{cr} = \int_0^1 F_2 x^* dx^* / \int_0^1 F_2 dx^* \tag{17}$$

$$\frac{dF_2}{dh_s^*} - A_1\frac{dF_2}{dh_s^*} = 0 \tag{18}$$

Performing the integration and differentiation gives

$$\alpha_{cr} = \frac{(\beta_{cr}+1)^3 - (\beta_{cr}+1)^{3/2}}{(\beta_{cr}+1)^3 - 1} \tag{19}$$

$$1 + (2\beta_{cr} - 1)(\beta_{cr}+1)^2 - 3\beta_{cr}(\beta_{cr}+1)^{1/2} = 0 \tag{20}$$

The critical shoulder height parameter β_{cr} can be obtained from equation (20) by the method of iteration. The critical riser location parameter α_{cr} is then evaluated from equation (19). Once the critical values α_{cr} and β_{cr} are determined, the optimal load-carrying capacity can be obtained. Since the pressure distribution of stepped bearings is linear over two steps, the optimal load capacity is equal to one-half of the maximum pressure at $x = \alpha_{cr} L$ multiplied by the bearing length. As a result, the dimensionless optimal load capacity is given by

$$W_{0op}^* = 0.5\alpha_{cr}\left[F_1(\beta_{cr}) - A_1 F_2(\beta_{cr})\right] \tag{21}$$

Dividing the shear force component acting upon the lower surface by the optimal load-carrying capacity results in the friction parameter.

$$\mu_{pop} = \frac{-F_0}{W_{op}} \cdot \frac{L}{h_{m0}} = \frac{-F_0^*}{W_{0op}^*} \tag{22}$$

where F_0^* represents the dimensionless shear force component acting upon the lower surface.

$$F_0^* = -\frac{\alpha_{cr}}{\beta_{cr}+1} - (1-\alpha_{cr}) - \frac{3\alpha_{cr}\beta_{cr}{}^2(1-\alpha_{cr})}{\alpha_{cr}+(1-\alpha_{cr})(\beta_{cr}+1)^3} \tag{23}$$

For the bearing undergoing a small perturbation, the perturbed film pressure is obtained by solving the perturbed equation (8). Following the procedure by Lu et al. [9], the dynamic stiffness coefficient and the damping coefficient under the optimal-load designing are given by:

$$S^* = \frac{c_{4r}(1-\alpha_{cr})^2 - c_{3r}\alpha_{cr}{}^2}{2} \tag{24}$$

$$D^* = \frac{c_{4i}(1-\alpha_{cr})^2 - c_{3i}\alpha_{cr}{}^2}{2} + \frac{(2-3\alpha_{cr}+\alpha_{cr}{}^3)(\beta_{cr}+1)^3 - \alpha_{cr}{}^3}{0.5(\beta_{cr}+1)^3} \tag{25}$$

where c_2 , c_{3r} , c_{3i} , c_{4r} and c_{4i} are

$$c_2 = \frac{-6\alpha_{cr}\beta_{cr}}{\alpha_{cr}+(1-\alpha_{cr})(\beta_{cr}+1)^3} \tag{26a}$$

$$c_{3r} = \frac{-3(1-\alpha_{cr})[c_1(\beta_{cr}+1)^2 - c_2]}{\alpha_{cr}+(1-\alpha_{cr})(\beta_{cr}+1)^3} \tag{26b}$$

$$c_{3i} = \frac{-6[(1-\alpha_{cr}{}^2)+\alpha_{cr}{}^2/(\beta_{cr}+1)^3]}{\alpha_{cr}+(1-\alpha_{cr})(\beta_{cr}+1)^3} \tag{26c}$$

$$c_{4r} = 3c_1(\beta_{cr}+1)^2 - 3c_2 + c_{3r}(\beta_{cr}+1)^3 \tag{26d}$$

$$c_{4i} = c_{3i}(\beta_{cr}+1)^3 \tag{26e}$$

4. Results and Discussion

From equation (20) the critical shoulder height parameter β_{cr} can be numerically calculated by the method of iteration. Using equation (19) the critical riser location parameter α_{cr} is therefore evaluated. According to the results, the optimal-load condition occurs at the situation: the critical shoulder height parameter $\beta_{cr} = 0.8437$ and the critical riser location parameter $\alpha_{cr} = 0.7003$. In order to display the steady performance and the dynamic characteristics under the optimal-load designing, four types of slider bearings including the plane profile by Lin et al. [7], the parabolic profile by Lin et al. [8], the stepped profile by Lu et al. [9] and the composite profile with $\alpha = 0.7$ by Lin et al. [10] are compared in this study.

The variation of dimensionless steady load-carrying capacity with shoulder height parameter β for different types of slider bearings is shown in Figure 3. Comparing with the plane-bearing case, an increment of the load is gained for the bearing with a parabolic film

shape. More over, larger load capacities are found for the composite bearing and the stepped bearing at medium values of the shoulder height parameter. Under the optimal-load designing, the stepped bearing with $\beta_{cr} = 0.8437$ and $\alpha_{cr} = 0.7003$ produces a maximum load-carrying capacity.

Figure 4 displays the variation of friction parameter with shoulder height parameter β for different slider bearings. Small differences of the friction parameter are found among the plane bearing, the parabolic bearing and the composite bearing, but the stepped bearing at medium shoulder height parameters results in a lower friction parameter. Under the optimal-load designing, the stepped-profile bearing at the critical condition $\beta_{cr} = 0.8437$ and $\alpha_{cr} = 0.7003$ predicts a smallest friction parameter.

Figure 5 presents the variation of dimensionless dynamic stiffness coefficient S^* with shoulder height parameter β for different types of slider bearings. Comparing with the plane-bearing case, the parabolic film shape signifies a higher value of the stiffness coefficient at high shoulder height parameters; but the composite bearing and the stepped bearing give a further increment of S^* for small values of β. Under the optimal-load designing, the stepped bearing at the optimal condition β_{cr} and α_{cr} provides a higher stiffness as compared to the plane bearing, the parabolic bearing and the composite bearing. However, the maximum stiffness of the stepped bearing occurs at a smaller shoulder height parameter than the case of optimal-load designing.

Figure 6 shows the variation of dimensionless dynamic damping coefficient D^* with shoulder height parameter β for different types of slider bearings. For all of the four types of bearings, the damping coefficient is observed to decrease with increasing β. Comparing with the stepped bearing, higher values of the damping coefficient are obtained for the plane bearing and, then, the composite bearing. In addition, the parabolic film shape is observed to produce the highest damping coefficient. Under the optimal-load designing, the bearing with the stepped profile at the condition of β_{cr} and α_{cr} predicts no contribution to the damping coefficient as compared to the plane bearing, the parabolic bearing and the composite bearing.

5. Conclusions

Based upon the theorem of calculus of variation, the optimal-load designing together with the dynamic characteristics of wide slider bearings with the gap height varying slowly is presented in this study. By applying the technique of calculus of variation, the optimization is achieved. According to the results and discussed, conclusions are drawn as follows.

Both of the steady-state performance and the dynamic characteristics are significantly affected by the film geometry and the shoulder height parameter of the bearing. By the technique of calculus of variation, the optimal-load condition occurs at a class of stepped bearings with the critical shoulder height parameter $\beta_{cr} = 0.8437$ and the critical riser location parameter $\alpha_{cr} = 0.7003$. Comparing with the cases of plane bearing, the parabolic bearing and the composite bearing, the stepped-profile bearing under the optimal-load

designing provides an enhancement in the load-carrying capacity, a reduction in the friction parameter as well as an improvement in the stiffness behavior. This optimal-load condition and the corresponding dynamic characteristics show useful information for engineers in bearing selection and designing.

6.References

1. Cameron, A., The Principles of Lubrication, Longmans Green & Co Ltd, London (1966).
2. Chowdhury, S.J., and Ahmadi, G., “Thermodynamic Analysis of Wide Thrust Bearings Operating in Laminar Inertial Flow Regimes,” ASME J. Lubrication Technology, Vol. 19, pp. 281-288 (1986).
3. Hamrock, B.J., Fundamentals of Fluid Film Lubrication, McGraw-Hill, Inc., New York. (1994).
4. King, K.F., and Taylor, C.M., “An Estimation of the Effect Fluid Inertia on the Performance of the Plane Inclined Slider Thrust Bearing with Particular Regard to Turbulent Lubrication,” ASME J. Lubrication Technology, Vol. 99, pp. 129-135 (1977).
5. Launder, B.E., and Leschziner, M.L., “Flow in Finite-width, Thrust Bearings Including Inertia Effects,” ASME J. Lubrication Technology, Vol. 100, pp. 330-338 (1978).
6. Lin, J.R., “Optimal Design of One-dimensional Porous Slider Bearings Using the Brinkman Model,” Tribology International, Vol. 34, pp. 57-64 (2001).
7. Lin, J.R., Lu, R.F., and Yang, C.B., “Linear Stability Analysis of a Wide Inclined Plane Slider Bearing,” Journal of Science and Technology, Vol. 10, pp. 349-354 (2001).
8. Lin, J.R., Lu, R.F, and Chien, R.D., “Steady and Dynamic Characteristics for a Wide Parabolic Slider Bearings,” Proceedings of 2004 Conference on the Tribology and Material Science, Huwei Institute of Technology, pp. 128-133 (2004).
9. Lu, R.F., Ho., M.H. and Lin, J.R., “A Study of Steady-state Performance and Dynamic Characteristics for Wide Rayleigh Step Slider Bearings,” Journal of Science and Technology, Vol. 14, No. 13, pp. 205-211 (2005).
10. Lin, J.R., Lu, R.F., Ho, M.H, and Lin, M.C., “Dynamic Characteristics of Wide Tapered-landed Slider Bearings,” Journal of the Chinese Institute of Engineers, Vol. 29, No. 3, pp. 543-548 (2006).
11. Pinkus, O., and Sternlicht, B., Theory of hydrodynamic lubrication, McGraw-Hill, New York (1961).
12. Qvale, E.B., and Wiltshire, F.R., “The Performance of Hydrodynamic Lubricating Films with Viscosity Variations Perpendicular to the Direction of Motion,” ASME J. Lubrication Technology, Vol. 94, pp. 44-48 (1972).
13. Rodkiewicz, C.M., and Anwar, M.I., “Inertia and Convective Effect in Hydrodynamic Lubrication of a Slider Bearing,” ASME J. Lubrication Technology, Vol. 93, pp. 313-315 (1971).
14. Rodkiewicz, C.M., Hinds, J.C., and Dayson, C., “Inertia, Convective, and Dissipation Effects in the Thermally Boosted Oil Lubricated Sliding Thrust Bearing,” ASME J. Lubrication Technology, Vol. 97, pp. 121-129 (1975).
15. Safar, Z. S., “Thermal and Inertia Effects in Turbulent-flow Thrust Bearing,” Proc. I. Mech. E., Vol. 22, pp. 43-45 (1980).

16. Synder, W.T., “The Nonlinear Hydrodynamic Slider Bearing,” ASME J. Basic Engineering, Vol. 85, pp. 429-434 (1963).
17. Taylor, C.M., and Dowson, D., “Turbulent Lubrication Theory - Application to Design,” ASME J. Lubrication Technology, Vol. 96, pp. 36-46 (1974).
18. Talmage, G., and Carpino, M., “A Pseudospectral-finite Difference Analysis of an Infinitely Wide Slider Bearing with Thermal and Inertia Effects,” STLE Tribology Transactions, Vol. 40, pp. 251-258 (1997).
19. Verma, P.D.S., Agrawal, V.K., and Bhat, S.B., “The Optimal Profile for a Porous Slider Bearing,” Wear, Vol. 48, pp. 9-14 (1978).

7.Figure and Table

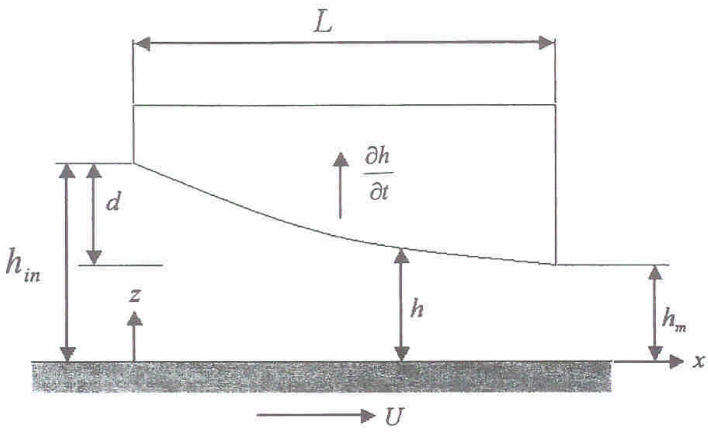

Figure 1 Geometrical configuration of a wide slider bearing with a curved profile

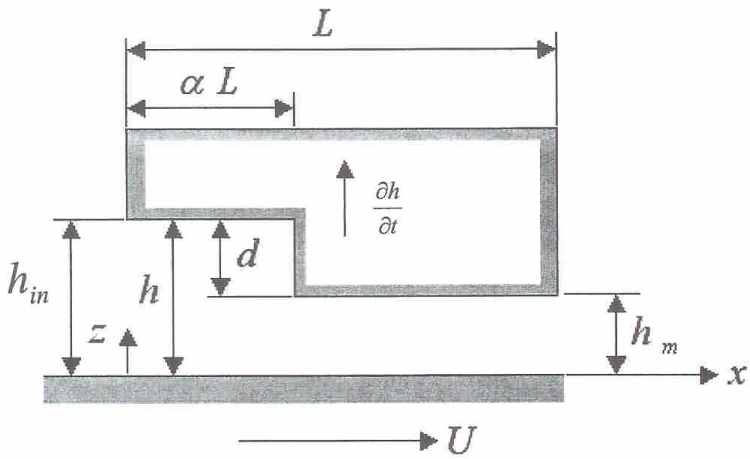

Figure 2 Geometrical configuration of a stepped-profile bearing with shoulder height d and riser location αL

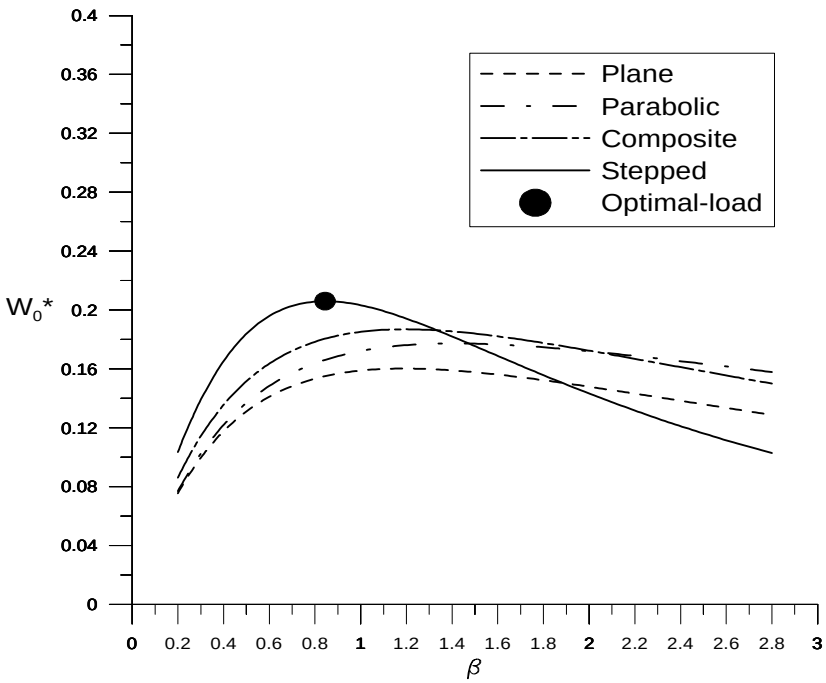

Figure 3 Variation of steady load capacity with shoulder height parameter for different types of bearings

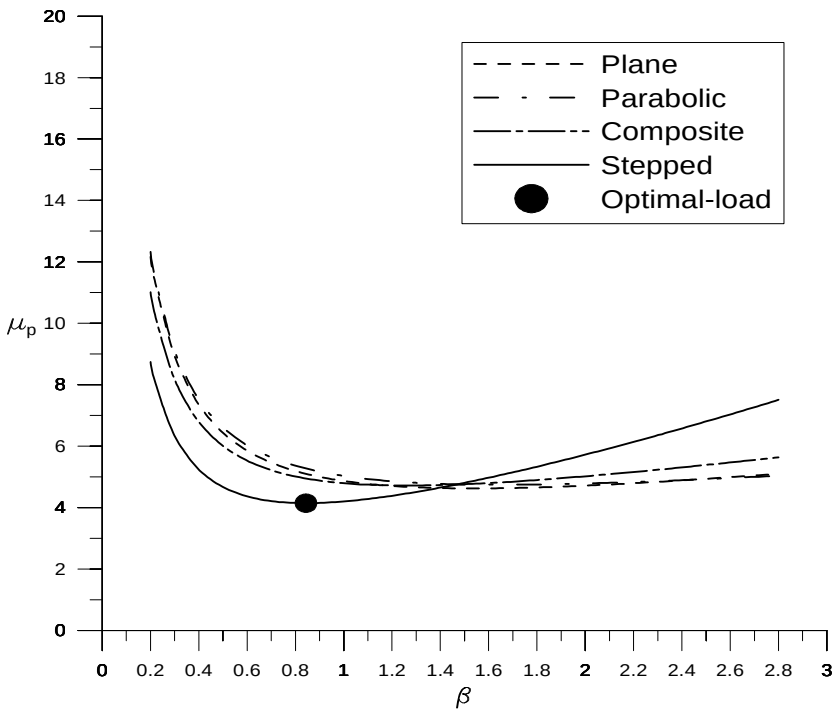

Figure 4 Variation of friction parameter with shoulder height parameter for different types of bearings

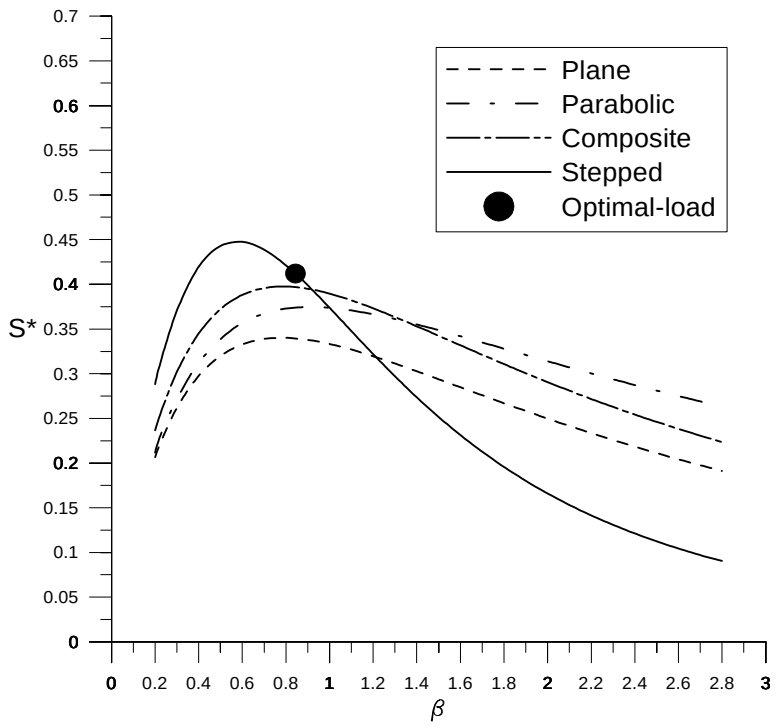

Figure 5 Variation of stiffness coefficient with shoulder height parameter for different types of bearings

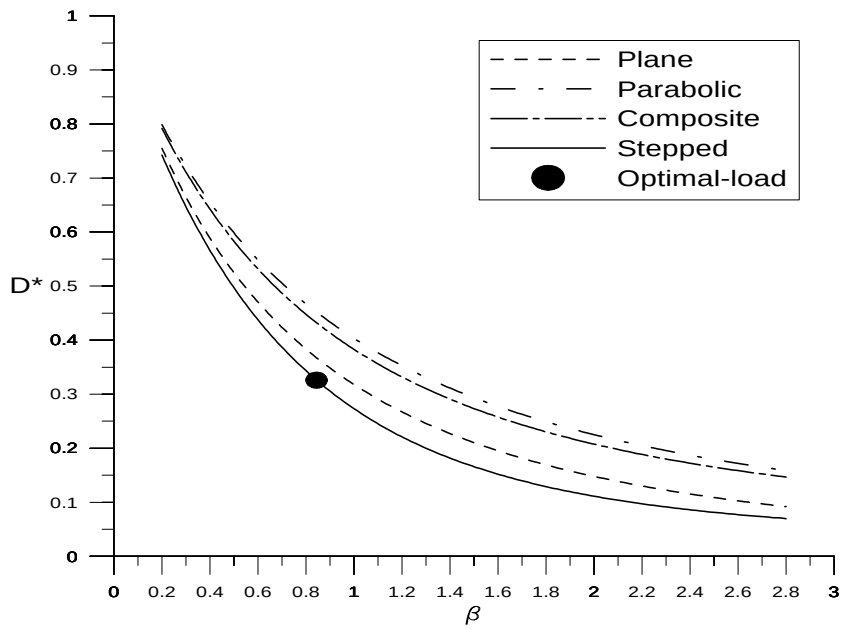

Figure 6 Variation of damping coefficient with shoulder height parameter for different types of bearing